Science of the Total Environment 839 (2022) 156385

Contents lists available at ScienceDirect

Science of the Total Environment

journal homepage: www.elsevier.com/locate/scitotenv

Investigating the sustainability of agricultural plastic products, combined influence of polymer characteristics and environmental conditions on microplastics aging

Gholamreza Bonyadinejad [a], Maryam Salehi [b,*], Amali Herath [a]

[a] Department of Civil Engineering, The University of Memphis, Memphis, TN, USA
[b] 108 Engineering Science Building, University of Memphis, Memphis, TN 38152, USA

HIGHLIGHTS

- Low molecular weight MPs are less photostable.
- LDPE covered by soil particles exhibited a lower rate of photodegradation.
- MPs surface oxidation is prominent under low relative humidity conditions.

GRAPHICAL ABSTRACT

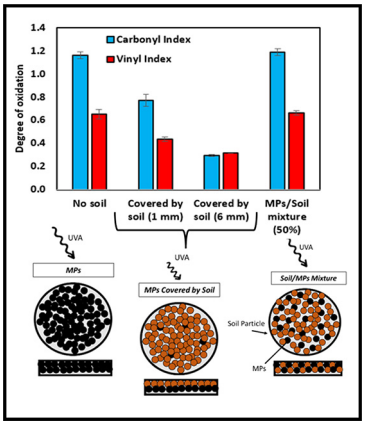

ARTICLE INFO

Editor: Damià Barceló

Keywords:
Microplastics
Photodegradation
Low density polyethylene
Agriculture
Soil health

ABSTRACT

The accelerated use of plastic products for agricultural practices has raised global concern regarding their negative impacts on soil health. This study aims to better understand the combined influence of polymer characteristics and environmental conditions on microplastic photodegradation within the agricultural soil system. For this purpose, the photodegradation behavior of low density polyethylene (LDPE) microplastics was studied through accelerated UVA radiation experiments under two different relative humidity (RH_{10} and RH_{70}) and soil deposition conditions. The variations of plastics' surface physiochemistry due to the accelerated photodegradation were studied using Attenuated Total Reflectance-Fourier Transform Infrared spectroscopy (ATR-FTIR), X-ray Photoelectron Spectroscopy (XPS), and Field Emission Scanning Electron Microscopy (FE-SEM). The carbonyl and vinyl indices were calculated using the ATR-FTIR information to compare the degree of microplastics' photodegradation. The plastics' bulk characteristics, including the percentage of crystallinity and molecular weight distributions, were examined using the Differential Scanning Calorimetry (DSC) and Gel Permeation Chromatography (GPC). Furthermore, the extent of UVA light interaction with the microplastics was studied by determining spectral quantum yield. The results demonstrated that new LDPE microplastics with a lower molecular weight (Mw = 233 kD) were subjected to a greater extent of photodegradation than those with greater molecular weight (Mw = 515 kD). Elevated relative humidity (RH_{70}) limited the photooxidation process of microplastics and consequently reduced the surface chemistry alterations. Deposition of soil particles with respect to the plastic particles impacted the photodegradation behavior. The microplastics covered by soil particles were not degraded, unlike those deposited next to the soil particles. The knowledge developed

* Corresponding author.
E-mail address: mssfndrn@memphis.edu (M. Salehi).

http://dx.doi.org/10.1016/j.scitotenv.2022.156385
Received 24 March 2022; Received in revised form 27 May 2022; Accepted 28 May 2022
Available online 31 May 2022

through this study could encourage the farmers and agricultural stakeholders to apply more efficient practices to remove plastic residuals after harvesting and conduct proper plastic disposal practices to protect soil health.

1. Introduction

Since the first use of plastic films as greenhouse covers in 1948, numerous plastic products ranging from mulch films to plastic encapsulated fertilizers have emerged to promote the productivity and efficiency of agricultural practices (Picuno and Mugnozza, 1994). Although global demand for greenhouse covers, mulching, and silage films is expected to rise by 50% from 6.1 million tonnes in 2018 to 9.5 million tonnes in 2030 (FAO, 2021), the concerns regarding the sustainability of these plastic products and their long term fate within the agricultural soil system still have not addressed. Having global food security compromised by soil pollution, it is critical to better understand the plastic pollutant fate within the farmlands. Agricultural plastic products undergo physiochemical deterioration as they expose to solar radiation, elevated temperature, mechanical forces, agrochemicals, and microorganisms (Shah et al., 2008; Manos et al., 2000). In many circumstances, multiple degradation mechanisms co-occur; however, typically, only one mechanism controls the decomposition rate. The chemical transformation caused by plastics' exposure to solar radiation makes plastics more brittle and susceptible to disintegration into the smaller particles called macroplastics (>5 mm), microplastics (100 nm-5 mm), and nanoplastics (<100 nm) (Horton et al., 2017; Ng et al., 2018). Fig. 1 demonstrates the plastic mulch residuals, macro and microplastics (MPs) extracted from the 3 cm topsoil after harvesting strawberries within agricultural farmland in Memphis, TN. Exposure of these plastic residuals to external physiochemical and biological factors such as solar radiation, abrasion with the soil particles, mechanical forces, and terrestrial organisms may further degrade and disintegrate the plastic particles. The recently published literature reported an extensive range of size distribution for MPs found within the agricultural farmland based on the sources of plastic release. For instance, most of the MPs found in soil treated with biosolids were fibers with median width and length of 20 μm and 0.97 mm, respectively (Corradini et al., 2019). Studying the soil samples from twenty vegetable fields in China revealed that plastic particles ranging from 20 μm to 5 mm as 78 and 62 items per kg in shallow (0–3 cm) and deep soils (3–6 cm) (Liu et al., 2018). The study conducted by Isari et al. (2021) revealed a greater accumulation of larger MPs (500 μm–5 mm) compared to the smaller MPs (20 μm–500 μm) within the soil samples collected from an agricultural field used for the cultivation of watermelons and canning tomatoes for over ten years (Isari et al., 2021).

MPs are considered an emerging threat to soil health as they may influence soil biophysics, geochemistry, and ecology (de Souza Machado et al., 2018). Recent studies have revealed overwhelming evidence of direct and indirect deleterious impacts caused by MPs pollution in the soil system (Rillig, 2012; Zhang et al., 2019; Wan et al., 2019; Kim and An, 2019; Liu et al., 2017). The MPs are anthropogenic stressors that may drive an alteration of a terrestrial ecosystem if they are not controlled properly. Despite the vast literature concerning MPs' contamination of aquatic systems (Wagner et al., 2018; Gallo et al., 2018; Mccormick et al., 2016), chemical degradation of MPs in agricultural soil has received less attention. Recent studies reporting the high accumulation of MPs in the farmland and soil systems are alarming, but only limited research has been conducted to examine the fate of MPs in the soil system. Direct ingestion of MPs by fauna may transfer them to the food chain. The MPs present within the farmland may influence the mobility of other contaminants such as pesticides and fertilizers within the soil profile (Hüffer et al., 2019). MPs impact the soil ecosystem through leaching of the plastics' plasticizers, additives, and degradation products or by interacting with biological components (de Souza Machado et al., 2018). Small MPs could be ingested by the fauna and accumulated in the food chain. The MPs could be the sink for other contaminants, as they can adsorb pollutants from the surrounding environment and locally concentrate them in the soil system (Rillig, 2012). The MPs' presence in the soil environment could alter the organic matter cycling and nutrient dynamics (Liu et al., 2017). MPs are also known to change water transport paths, reduce infiltration rate and increase contaminant transport velocity (Jiang et al., 2017). Although the MPs' biological degradation and transport via the terrestrial organisms and microorganisms have been well investigated, their chemical and physical changes due to the solar radiation have received less attention. However, the variation of MPs'

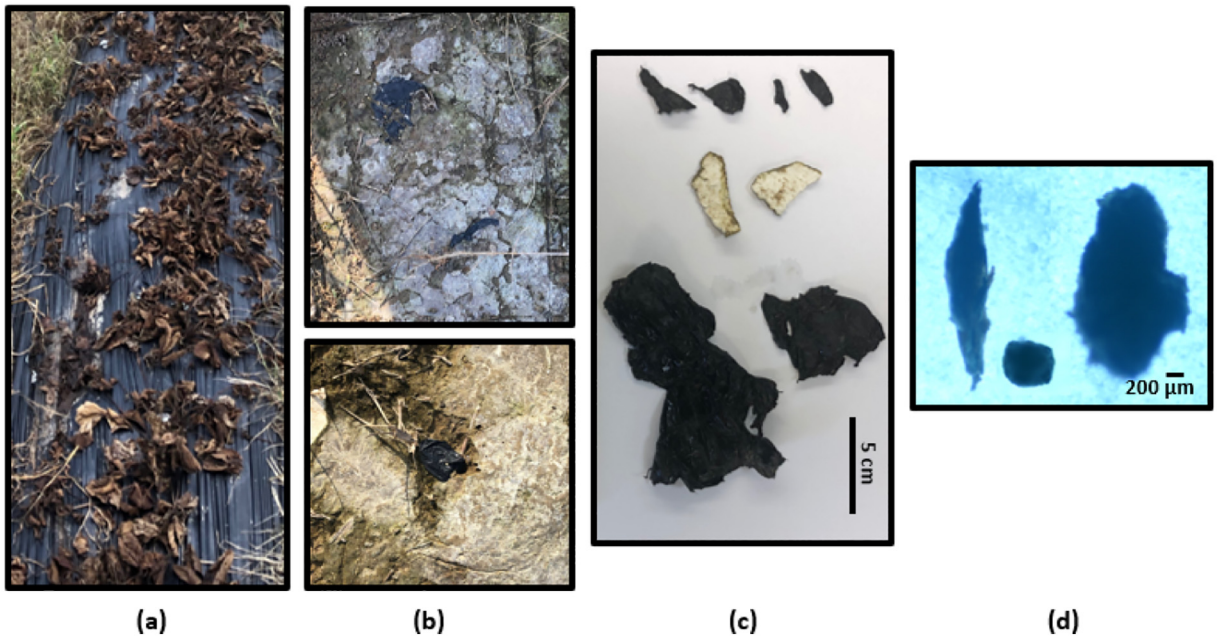

Fig. 1. (a) Plastic mulch remained within the farmland after harvesting the strawberries in a field located in Memphis, TN (2019), (b) plastic mulch residuals and (c) macroplastics found within the topsoil, and (d) optical microscopy images of microplastics extracted from the topsoil.

surface chemistry due to environmental degradation may influence their interaction with other agrochemicals present within the soil. Our previous studies demonstrated that with the aging of plastics, the surface polarity increases, and a greater level of heavy metals gets accumulated on their surface (Hadiuzzaman et al., 2022; Aghilinasrollahabadi et al., 2021; Huang et al., 2019). Thus, a greater level of contaminant could be transported by aged MPs to the deep soil, which endangers the terrestrial organisms.

A recent UN report has estimated 34% of agricultural films as mulch (FAO, 2021). Low density polyethylene (LDPE) is the major polymer used to generate regular and non-biodegradable plastic mulch (Dilara and Briassoulis, 2000; Steinmetz, 2016; Kapanen et al., 2008). Extensive studies investigated photooxidation of polyolefin greenhouse covers (Dehbi et al., 2010; Ali et al., 2016) and revealed the formation of carbonyl (—C═O), vinyl (—C═C), and hydroxyl bonds (—OH) on their surface. However, information regarding the further degradation of plastic residuals left within the topsoil has not been studied yet. External substances such as soil particles and plant pieces could accumulate on the plastic surface as they expose to solar radiation. The chemical and physical changes caused by these external objects could impact the photodegradation of MPs (Richard et al., 2019). The disintegration of plastic segments into smaller particles increases their surface area. However, information regarding the influence of plastic mulch disintegration on their photodegradation behavior is lacking. Thus, this study aims to better understand the combined physicochemical factors that influence plastic residuals' photodegradation within the agricultural soil system. The specific objectives are to (1) correlate the MPs' photodegradation behavior to their microstructure and environmental conditions, (2) characterize the MPs surface physiochemistry and bulk characteristics variation due to the accelerated photodegradation, and (3) examine the extent of UVA light and MPs interaction by determination of spectral quantum yield.

2. Experimental

2.1. Materials

The LDPE materials were selected for this study due to their widespread applications for plastic mulching silage films, irrigation pipes, and greenhouse covers (Dilara and Briassoulis, 2000; Steinmetz, 2016; Kapanen et al., 2008). LDPE powder was purchased from Alfa Aesar (Cat No. 42607). Metallic sieves (No.35, No.50, and No.140) were used to collect the LDPE particles of $d_p < 106$ μm (hereafter 106 μm) and 300 μm $< d_p <$ 500 μm (hereafter 400 μm) according to the ASTM method D1921. It should be noted that the size distribution and microstructure of MPs released to the topsoil could be highly different from various sources. Despite the wide range of sizes for MPs found within the farmlands, we have limited our study to those smaller than 106 μm and between 300 μm and 500 μm as they are more susceptible than larger particles to transport into the deep soil. Thus, the changes in their surface chemistry caused by the photodegradation would be more critical in terms of impacts on the terrestrial organisms. The sieve analysis revealed the particle size for the soil used in this study is between 425 μm and 1000 μm, which falls into the sandy soil category (20 μm–2 mm). Globally, sandy soil covers around 31% of the entire land. The major regions with the sandy soil are located along the margins of continents, including northern Europe, North America, Asia, South America, and Africa. About 199,600,000 ha of the sandy soils are utilized as farmlands (Petersen et al., 2016; Huang and Hartemink, 2020). As suggested by the literature, the soil was pretreated by three times rinsing with water, followed by heating at 450 °C for 4 h in an A1400 Thermolyne Muffle furnace to remove the external organic contaminant (Song et al., 2017). The reason for this pretreatment was to exclude the soil organic contents' influence on the photodegradation process. The objective of this study was only to examine the influence of soil particles as the physical barriers in reaching the UV radiation to the MPs. Water used in the experiments was treated with Ultrapure Milli-Q-IQ 7000.

2.2. Accelerated photodegradation experiments

For this purpose, the plastic particles (106 μm and 400 μm) were evenly distributed with 1 mm thickness in glass Petri dishes of 10 cm. The plastic particle samples were placed in a QUV weathering tester for the varied duration of UVA exposure. A UV-AB meter (Anaheim Scientific M150 Mini UV-AB Meter, Wilmington, NC, USA) was utilized to measure the real-time irradiation intensity of UVA bulbs. The eight UVA fluorescent lamps in the QUV weathering tester generated a UVA light of 340 nm at 6.3 ± 0.3 mW/cm^2. The Petri dishes containing plastic particles were repositioned every 24 h for even exposure of plastic particles to UVA irradiation. Before any analysis, the plastic particles present in each Petri dish were completely mixed. The UVA exposure was conducted under the relative humidity of <10% (RH_{10}) and 70 ± 2% (RH_{70}) to examine the influence of humidity on the photodegradation behavior of plastics. An Inkbird ITH-20 humidity meter was used to monitor the relative humidity inside the weathering chamber. The RH_{10} and RH_{70} were achieved through irradiation/dark and irradiation/condensation cycles, respectively. The irradiation cycle was 8 h followed by 2 h of either dark or condensation cycle. The temperatures during irradiation and dark/condensation cycles were 51 °C and 40 °C, respectively. The mixtures of soil and MPs particles were exposed to UVA radiation for 3 w to study the influence of MPs deposition within the soil structure on their photodegradation behavior. The MPs with an average diameter of 400 μm that were exposed to UVA radiation for 5.2 w (RH_{10}) are referred 5 w UVA exposed MPs in the paper. The MPs and soil were mixed and placed in 1.0 mm thickness in a glass Petri dish uniformly. The influence of soil content in MPs/soil mixture on photodegradation behavior of MPs was investigated using four different MPs/soil mass ratios of 25, 50, 75, and 100 *w*/w%. At the end of each exposure period, the MPs/soil content of each petri dish was completely mixed by placing the lid on and shaking; then, MPs were separated from the soil using gravity separation. The separated MPs were subjected to different characterization practices.

2.3. Plastics characterization

2.3.1. Surface chemistry analysis

The ATR-FTIR absorption spectra were recorded from 4000 to 400 cm^{-1} with a 4 cm^{-1} resolution using a Thermoscientific ATR-FTIR spectrophotometer (Nicolet Summit FTIR with an Everest ATR) equipped with a diamond crystal. In this study, the degree of plastics photodegradation was evaluated by calculating the carbonyl index (CI) and vinyl index (VI) according to the Eqs. (1) and (2), where A_{1715}, A_{2870}, and A_{909} are the absorbances of carbonyl, methylene, and vinyl bonds, respectively (Salehi et al., 2018; Babaghayou et al., 2016):

$$CI = A_{1715}/A_{2870} \quad (1)$$

$$VI = A_{909}/A_{2870} \quad (2)$$

XPS analysis was conducted for new and UVA exposed LDPE MPs to attain a more surface-specific quantitative analysis of atomic ratios of oxidized carbon functional groups created due to the photodegradation. A K-Alpha Thermo Scientific Spectrophotometer X-ray photoelectron spectroscopy (XPS) with monochromatic Al Kα radiation ($h\upsilon$ = 1486.6 eV) was employed for the XPS analysis in which the X-ray power of 75 W at 12 kV with a spot size of 400 μm^2 was used. The K-Alpha instrument had a base pressure of 1.0×10^{-9} mBa. Au 4f7/2 at 84.0 eV and Cu 2p3/2 at 932.67 eV were used for calibration instrument. The spectra calibration was conducted using the C 1s line of the absorbed hydrocarbon layer, which has a binding energy of 284.6 eV. The "Avantage v5.995" software that came with the instrument was used to collect XPS data.

2.3.2. Surface morphology analysis

The field emission scanning electron microscopy (FE-SEM) and water contact angle analysis were conducted to examine the MPs' surface

morphology. The FE-SEM instrument was FEI Nova Nano SEM 650 equipped with an Oxford X-Max^N Silicon Drift detector. It functioned with an 18-kV electron accelerating voltage at a 5.0 mm distance from the plastic surfaces. The maximum penetration depth and the depth of the maximum signal at 18KV were about 4 μm and 2 μm, respectively. Before analysis, the samples were coated with a 5 nm layer of conductive Gold/Palladium in a 60:40 ratio under a high vacuum using an EMS 550× sputter coater to avoid surface alteration during imaging.

2.3.3. Bulk material characterization

The Differential Scanning Calorimetry (DSC) analysis was conducted for new and photodegraded MPs using a TA Instrument Model Q20 V24.11. Indium standard was employed for the instrument calibration. The MPs and LDPE film samples were heated from 0 °C at a heating rate of 10 °C/min to 150 °C and subsequently cooled to 0 °C at the same rate using a nitrogen atmosphere with a flow rate of 50 ml/min. The transition temperature and the degree of crystallinity were determined using the TA Universal Analysis software. For each measurement, 4 to 6 mg of samples were placed in a standard aluminum pan. The degree of crystallization was calculated from the first heating experiment, using Eq. (3), where ΔHm is the melting enthalpy of the sample and ΔH_m^{ref} is the melting enthalpy of 100% crystalline polymer. The ΔH_m^{ref} was considered as 293 J/g for PE. The melting enthalpies were measured using a sigmoidal baseline (Canopoli et al., 2020).

$$Crystallinity\ (\%) = \frac{\Delta Hm}{\Delta H_m^{ref}} \times 100 \tag{3}$$

The Gel Permeation Chromatography (GPC) analysis was conducted to identify the degree of molecular weight variations due to the MPs' photodegradation. Number average molecular weights (M_n), weight average molecular weights (M_w), and peak molecular weight (M_p) of new and UVA exposed MPs were compared. The number average molecular weight (M_n) is the statistical average molecular weight of all the polymer chains in the sample and is calculated according to Eq. (4), where M_i is the molecular weight of a chain and N_i is the number of chains with that molecular weight.

$$Mn = \frac{\sum NiMi}{\sum Ni} \tag{4}$$

M_w takes into account the molecular weight of a chain in determining contributions to the molecular weight average. The more massive chain, the more the chain contributes to M_w. The weight average molecular weight is calculated according to Eq. (5), and Mz is calculated according to Eq. (6).

$$Mw = \frac{\sum NiMi^2}{\sum NiMi} \tag{5}$$

$$Mz = \frac{\sum NiMi^3}{\sum NiMi^2} \tag{6}$$

The M_z average molecular weight is more sensitive to the greater molecular weight of polymeric chains and consequently is more difficult to be measured with accuracy. This order of magnitude is present for all synthetic polydisperse polymers: $M_n < M_w < M_z$. The peak molecular weight (M_p) is defined as the molecular weight of the highest peak. Therefore, M_p is the mode of the molecular weight distribution. For this purpose, a PL-SP260 high temperature sample preparation system was utilized to prepare the sample solutions in 1,2, 4-trichlorobenzene (TCB) as polymeric solvent. The samples were heated to 160 °C and left to be dissolved for 2 h, followed by a gradual stirring for 10 min to achieve a homogenous polymeric solution. The analysis was conducted using a Viscotek 350B HT-GPC from Malvern Instruments equipped with a Viscotek TDA 305 detector suite with integrated refractive index, light scattering (830 nm at 90° and 7°), and differential viscometer detectors. The system was equipped with a 200 μL injection sample loop and CLM6210-HTx3 three column set from Malvern operated at 150 °C with a flow rate of 1 ml/min. Malvern's OmniSEC software was employed to analyze the data. For triple detection, a polystyrene narrow standard was used to set the calibration constants used in the OmniSEC GPC software.

2.4. Quantum yield calculation

Light energy absorbed by a molecule upon irradiation can be dissipated into photophysical or photochemical reactions. The functional groups present in the singlet ground state of the polymer are excited into a singlet excited state by absorbing a quantum of light. This energy can be released by returning to the singlet ground state through fluorescence or internal conversion. Besides that, intersystem crossing can occur by inverting the spin and transferring it into an excited triplet state followed by phosphorescence. But these photophysical reactions are unlikely to occur at elevated temperatures. In contrast, photochemical processes such as molecular rearrangement, free radical formation, and photoionization dominate even at room temperature. These types of chemical reactions can take place either from excited singlet or triplet state (Guillet, 1973; Guillet and Dan, 1973). The generation of free radicals and their propagation within the molecule causes polymer chain scission. This leads to reducing the molecular weight of the polymer by increasing the irradiation duration. Ultimately this causes the polymer to deteriorate and degrade. The efficiency of polymer photodegradation due to UVA irradiation can be measured in terms of quantum yield. This study calculated the quantum yield for chain scission by the differences in molecular weight of new and UVA exposed LDPE MPs. All UVA radiation is not absorbed by polymer. Moreover, all absorbed radiation does not photolitically degrade the polymer. To better understand the efficiency of this photolytic process, the quantum yield (ϕ_{CS}) for the chain scission of LDPE films under different UVA irradiation durations was calculated according to Eq. (7), where (η_0) and (η_t) are the intrinsic viscosities of the polymer (dL/g) obtained before and after UVA irradiation. m, α, M_{no}, and I denote the mass of the polymer irradiated (g), Mark-Houwink parameter constant related to polymer viscosity, number average molecular weight of LDPE before UV irradiation, and the incident intensity of UVA (1.8×10^{-4} ein m^{-2} s^{-1}), respectively (Guillet and Dan, 1973). The average number of chain scissions (N) in terms of an average number of cuts per single chain was calculated using the Eq. (8). The chain scission highly depends on the number average molecular weight before (M_{no}) and after (M_{nt}) photoirradiation (Angulo-Sanchez et al., 1994). The data for the above parameters were obtained by the results of GPC analysis.

$$\phi_{CS} = \frac{m\left[(\eta_0/\eta_t)^{1/\alpha} - 1\right]}{M_{no} I} \tag{7}$$

$$N = \frac{M_{no}}{M_{nt}} - 1 \tag{8}$$

3. Results and discussion

3.1. Surface chemistry variation

3.1.1. The ATR-FTIR analysis

The ATR-FTIR spectroscopy analysis of photodegraded LDPE particles (d_p = 400 μm) revealed remarkable surface chemistry changes compared to the new MPs (Fig. 2). The absorption bands at 2914 cm^{-1} and 2847 cm^{-1} on new LDPE particles demonstrate the >CH stretching. However, as early as 3 w of UVA exposure, a new absorbance peak has appeared at the wavenumber of 1712 cm^{-1}, corresponding to carbonyl (>C═O) functional groups (Roff, 1956; Jung et al., 2018). The absorbance peak that appeared at 909 cm^{-1} demonstrates the formation of the vinyl group (>C═C<) due to the UVA exposure. The carbonyl and vinyl indices for photodegrade MPs were increased linearly with increasing UVA exposure duration. Fig. 3 demonstrates the degree of LDPE MPs oxidation in terms

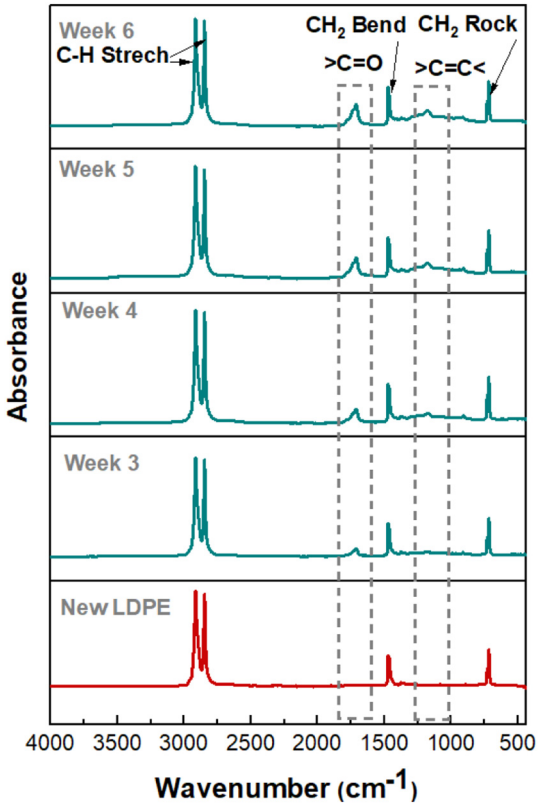

Fig. 2. ATR-FTIR spectra of new and UVA exposed LDPE MPs (d_p = 400 μm, $RH_{70,}$ no soil).

of CI and VI growth over the UVA exposure duration under RH_{70} conditions when the soil was absent. The generation of the carbonyl group can be explained by the mechanism of the LDPE photodegradation. The LDPE photodegradation is photooxidation caused by the formation of free radicals during the initiation process. The UV radiation causes breakage of >C—C< and >C—H bonds present in LDPE (Singh and Sharma, 2008). The produced free radicals caused by cleavage of >C—H and >C—C< bonds can react with available oxygen and create carbonyl groups (>C═O) via chain propagation, chain termination, chain branching, cross-linking, and chain scission processes (Ranjan and Goel, 2019). A similar ATR-FTIR spectrum was found for LDPE MPs with a diameter of 106 μm, after 3 w UVA exposure (Fig. 4). Comparing the 3 w photodegraded MPs with the diameter of 400 μm and 106 μm (RH70, no soil) revealed a greater extent of photodegradation for larger LDPE MPs than to the smaller MPs. The vinyl and carbonyl indices were found as 0.5 and 0.6 for larger MPs; however, they were found as 0.4 and 0.5 for

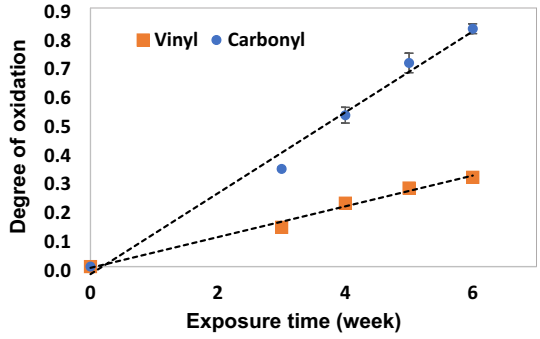

Fig. 3. The growth of carbonyl and vinyl indices over time for LDPE MPs (d_p = 400 μm, RH_{70}, no soil).

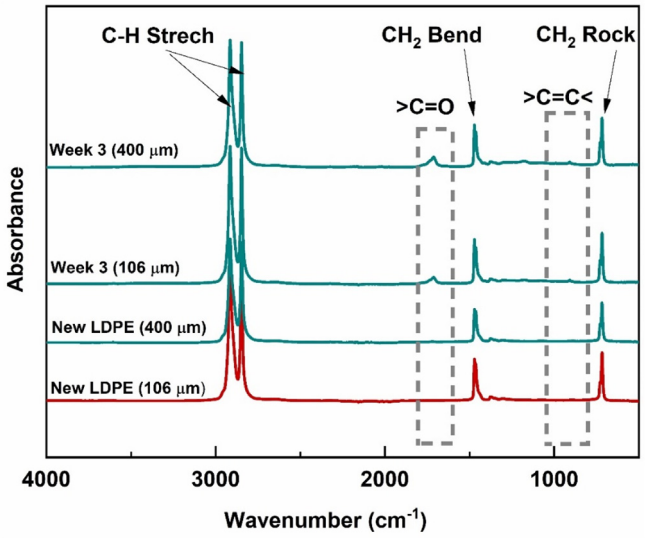

Fig. 4. ATR-FTIR spectra of new and 3 w UVA exposed LDPE MPs (d_p = 106 μm and 400 μm, $RH_{70,}$ no soil).

smaller LDPE MPs. No prior study was found investigating the role of MPs' size distribution on their photodegradation behavior; however, few studies that investigated the photostability of inorganic particles [e.g., TiO_2, ZnO] as a factor of their size distribution have underscored the role of particles' intrinsic characteristics, surface area, particle-to-particle distance on their light scattering and UV absorbance behavior (Goh et al., 2014; Egerton, 2014; Kockler et al., 2014). Despite the Kockler et al. (2014) findings of increased photodegradation for smaller TiO_2 particles due to their greater surface area, in this research, we found a lower extent of photodegradation for smaller plastic particles (Kockler et al., 2014). Thus, it was inferred that MPs' intrinsic characteristics may have contributed to their photostability. Further GPC analyses were conducted to better understand the reasons behind the different degradation behavior of these two plastic sizes by characterizing their molecular weight distributions as explained in Section 3.3.1.

3.1.1.1. The impact of MPs deposition within the soil structure. Deposition of MPs with respect to the soil particles impacted their photodegradation behavior. The plastic particles covered by soil were not degraded, unlike those placed next to the soil particles. As shown in Fig. 5, the soil particles were placed adjacent to the MPs in the soil/MPs uniform mixtures; however, the soil particles covered the MPs completely in the layered deposition. The ATR-FTIR analysis of LDPE MPs (106 μm and 400 μm) mixed with different amounts of soil (25%, 50%, 75% MPs/soil *w*/w%) exposed to the UVA radiation for 3 w (RH_{10} and RH_{70}) revealed no significant changes of CI and VI indices compared to those MPs photodegraded under a similar condition in the absence of soil. The greatest CI and VI increments (0.89 and 0.34) were found for MPs (d_p = 400 μm) mixed with soil (50% MPs/soil w/w%, RH_{10} condition) after 5 w of UVA exposure. However, these values were not significantly different from those MPs photodegraded in the absence of soil. The lack of significant surface chemistry differences of the MPs that were uniformly mixed with soil can be inferred from the neutral role of soil particles as an inhibitor on initiating reactions. In the uniform mixture of soil/MPs, the soil grains were placed next to the MPs and did not cover those.

On the other hand, the coverage of MPs by soil particles (soil layer thickness of 1, 3, and 6 mm) hindered the UVA exposure of MPs through the photodegradation experiments. No degree of oxidation was identified for MPs covered by a 6 mm soil layer after 5 w of UVA exposure. The CI and VI were increased more significantly (0.47 and 0.12) for MPs covered by 1 mm soil layer compared to those that were covered by 3 mm soil (CI = 0.09 and VI = 0.03). Barnes et al. (2012) reported a similar result regarding

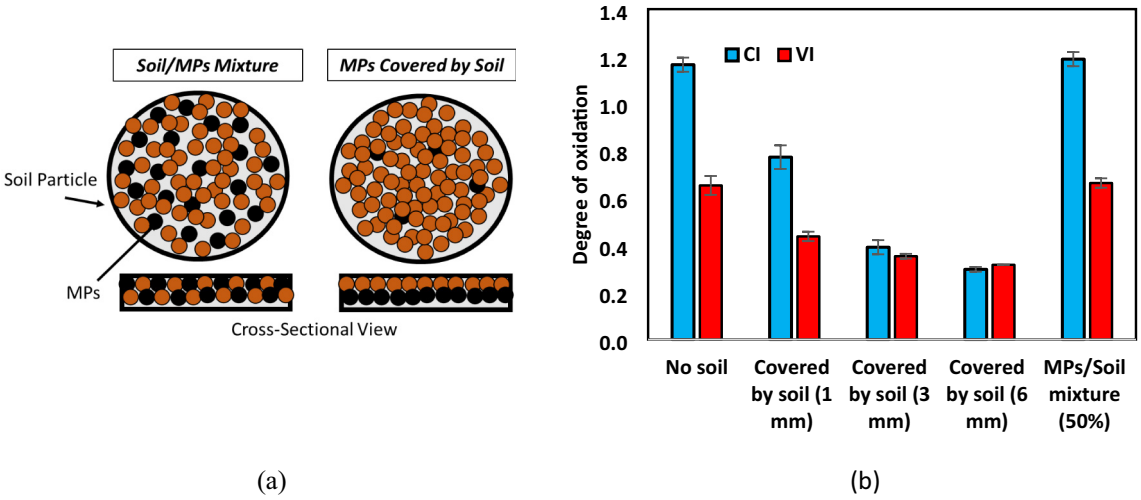

Fig. 5. (a) schematic demonstrating the two different depositions of MPs and soil particles, (b) the carbonyl (CI) and vinyl indices (VI) for MPs present in different depositions in respect to the soil particles.

the hindering influence of soil coverage on the photodegradation process. This investigation further clarified that, however, the accelerated photodegradation experiments were conducted at 51 °C, but the thermal degradation has not contributed to the MPs degradation as the MPs covered by soil did not demonstrate any surface chemistry alteration despite experiencing this temperature. Although having the MPs buried within the soil column reduces their photodegradation, it could facilitate their soil-mediated degradation processes due to the greater contact with the soil organisms, water, and agrochemicals.

3.1.1.2. The influence of relative humidity. ATR-FTIR analysis demonstrated that photodegradation of MPs (both 400 μm and 106 μm) occurred to a greater extent under lower relative humidity (RH_{10}) compared to the elevated relative humidity (RH_{70}) condition. The more significant CI and VI increments (0.86, 0.33) were found for LDPE MPs (400 μm) due to 5 w of UVA exposure in RH_{10} condition compared to the RH_{70} (0.70 and 0.28) when the soil was absent. A similar trend was found for the samples containing the uniform MPs/soil mixture. The lower degree of MPs photodegradation under elevated relative humidity conditions can be ascribed to either role of water drops (as the water vapor is settled on the surface of the particles during the condensation cycle) or as an oxygen barrier or as a UV refractor (Dilara and Briassoulis, 2000; Gewert et al., 2015). To illustrate the role of water drops as an oxygen barrier, it is worthwhile to mention that during the propagation phase, oxygenated low molecular weight fragments are formed due to autoxidation. Therefore, during this process presence of oxygen is essential since oxygen is incorporated into the polymers (Gewert et al., 2015). Thus, with the constant light intensity and low available oxygen, the oxygen uptake rate is proportional to the concentration of oxygen present at any given time. In this case, oxygen is the limiting factor and therefore controls the rate of photodegradation. A future systematic investigation is needed to distinguish the role of reduced oxygen content from UV refraction in reducing the extent of photodegradation.

3.1.2. X-ray Photoelectron Spectroscopy (XPS)

XPS analysis was conducted for new and UVA exposed LDPE MPs to attain a more quantitative analysis of surface chemistry variation due to the photodegradation. The elemental atomic surface concentrations for new and photodegraded LDPE MPs are listed in Table SI-1. As can be seen in the Fig. 6a, no oxygen was detected on the surface of MPs (d_p = 400 μm, RH_{10}, no soil), but a dominant peak at the binding energy of 284.8 eV, which is associated with the main feature of LDPE structure (>C—C<) (Salehi et al., 2018). Although, the peak at the binding energy of 284.8 eV is still dominant for MPs that were photodegraded for 3 w and 5 w (Fig. 6b). The new peak at the binding energy of 531.9 eV corresponding to O1s was found on 3 w, and 5 w UVA exposed MPs and confirmed the photooxidation (Salehi et al., 2018). The atomic percentage of O1s increased to 4.4% and 7.1% for 3 and 5 w UVA exposed MPs, respectively. The high resolution C1s spectrum for LDPE MPs was deconvoluted to identify the atomic surface concentrations of different carbon oxidation states. Four peaks at the binding energies of 284.7 eV, 286.4 eV, 287.7 eV and 289.2 eV were identified corresponding to >C—C<, >C—O, >C═O and >O—C═O functional groups, respectively (Salehi et al., 2018). Unlike the >C—C< content, the atomic surface concentration of >C—O, >C═O, and >O—C═O have increased from 0.6%, 0.4%, and 0.1% to 14.6%, 4.2%, and 0.7% with increased duration of UVA exposure from 3 w to 5 w. It demonstrates a progressive photodegradation over time.

3.2. Surface morphology alteration

To evaluate the surface morphology alteration of photodegraded LDPE MPs, new and 5 w UVA exposed MPs were studied through FE-SEM imaging (Fig. 6). The surface cracks have appeared in 5 w UVA exposed MPs. The crack formation can be attributed to the chain scission followed by chemicrystallization phenomenon. Due to the kinetic regulation of oxygen diffusion, oxidation is limited to a superficial layer, leading to oxidation-induced surface cracks (Zahra, 2014; Colin and Verdu, 2012).

3.3. The variations of MPs' bulk characteristics

3.3.1. Molecular weight variations

As shown in Table 1, the smaller LDPE MPs (d_p = 106 μm) had greater molecular weights than larger MPs (d_p = 400 μm). This finding explains the greater extent of photodegradation for larger MPs compared to the smaller MPs, as described in Section 3.1.1. Despite the greater average molecular weight of the new 106 μm diameter particles, its peak molecular weight ($M_p = 62 \times 10^3$) was smaller than the peak molecular weight for the new 400 μm diameter particles ($M_p = 71 \times 10^3$). This finding demonstrates the broader molecular weight distribution for the polymeric chains within the new 106 μm diameter particles compared to the new 400 μm diameter particles. Thus, despite a smaller mode of molecular weight distribution, the presence of very long polymeric chains resulted in a greater average molecular weight for 106 μm diameter particles.

The calculation of the polydispersity index using Eq. (9) also confirmed a broader molecular weight distribution for new 106 μm diameter particles compared to the new 400 μm diameter particles. The difference in the molecular weights for the plastic particles could be due to the manufacturing process where the greater molecular weight polymer was disintegrated into smaller particles. Future investigation is needed to study the link

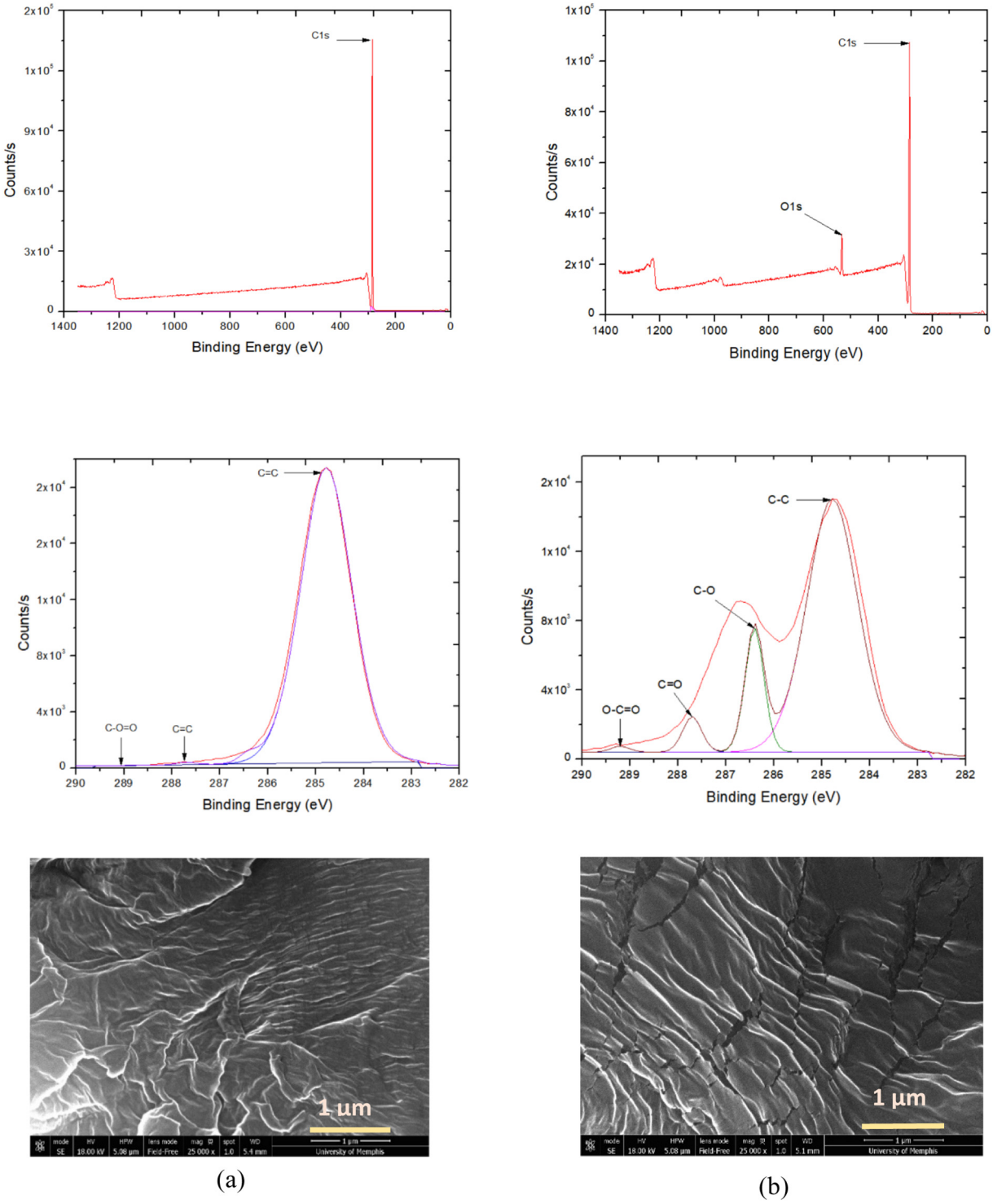

Fig. 6. The survey and C1s high resolution XPS spectra and FE-SEM images of (a) new and (b) 5 w UVA exposed MPs (RH_{10}, d_p = 400 µm, no soil).

between the fragmentation behavior of plastics and their microstructure characteristics.

$$\text{Polydispersity Index} = \frac{M_w}{M_n} \tag{9}$$

Both size distributions of MPs revealed a greater than 90% reduction of their M_p upon 3 w of UVA exposure. Furthermore, the M_n and M_w of all studied MPs reduced by over 84% after 3 w of UVA exposure. The greatest percent reduction in M_p (94.7%) was found for 5 w UVA exposed MPs (d_p = 400 µm) under RH_{10} condition. The M_n and M_w of MPs (d_p = 400 µm) were reduced to a greater extent by increasing the UVA exposure from 3 w to 5 w under a low relative humidity condition (RH_{10}). However, the MPs (d_p = 400 µm) that were photodegraded under elevated relative humidity (RH_{70}) demonstrated the increased M_n and M_w from 2.94 × 10^3 and 25.1 × 10^3 to 6.41 × 10^3 and 26.2 × 10^3 by increasing the UVA exposure from 3 w to 5 w, respectively. The significant drop in MPs molecular weight during the first stage (3 w) of UVA exposure under both relative humidity conditions is attributed to the chain scission reactions. However, increasing the molecular weight during the second stage (3 w

Table 1
The molecular weights for new and UVA exposed LDPE MPs.

LDPE MPs	Condition	UVA exposure duration (w)	$M_p \times 10^3$	$M_z \times 10^3$	$M_n \times 10^3$	$M_w \times 10^3$
d_p = 400 μm	New	0	71.0	2906.0	41.5	233.0
	RH_{10}	3	6.1	506.9	6.5	27.0
		5	3.8	30.4	4.92	8.8
	RH_{70}	3	5.6	180.7	2.9	25.1
		6	6.4	163.5	6.4	26.2
d_p = 106 μm	New	0	62.0	4502.0	55.2	515.0
	RH_{10}	3	3.8	126.4	0.9	21.2

and 5 w) under RH_{70} conditions can be ascribed to cross-linking reactions (Angulo-Sanchez et al., 1994; Berlanga-Duarte et al., 1996; Rodriguez et al., 2020; David et al., 1992). Indeed, photodegradation of polymers causes chain scission and cross-linking, with the former being more prevalent in the presence of oxygen. The chain scissions result in a decrease in both M_n and M_w in the absence of cross-linking. However, there will be an increase in molecular weight and microstructure alteration (branching crosslinking and gel formation) if cross-linking is the primary process (Berlanga-Duarte et al., 1996; David et al., 1992). As polymeric chain scission reaction begins and becomes pervasive, the vinyl groups may form according to Norrish type II process. This vinyl formation process occurs after the formation of carbonyl groups and chain scissions in their vicinity, which subsequently reduces molecular weight (Babaghayou et al., 2016). Different sources, including the plastic mulch, silage films, greenhouse covers, irrigation pipes, and plastic containing fertilizers, could contribute to the MPs release. Thus, the size distribution and microstructure of MPs found within the topsoil could be highly different. Understanding the link between MPs' physical characteristics and photodegradation behavior could promote more informed agricultural management practices.

3.3.2. Crystallinity variations

LDPE is a semicrystalline polymer and it's crystalline phase called spherulites is separated by amorphous regions (Dilara and Briassoulis, 2000). Neighboring crystalline lamellae are connected by tie molecules, passing through the amorphous interlamellar regions. The LDPE oxidation is constrained to the amorphous area (Sebaa et al., 1993). The DSC results, including the melting peak temperature T_p (C°), melting enthalpies ΔH (J/g), and crystallinities percentage, are presented in Table SI-2. The % crystallinity was almost similar for new 106 μm (24.4%) and 400 μm (24.7%) LDPE MPs. The crystallinity of new MPs for d_p = 106 μm is 24.4% and for d_p = 400 μm is almost similar (24.7%). However, after 3 w of UVA exposure, the crystallinity of larger particles has increased to a greater extent than smaller particles. The percent crystallinities for particles with d_p = 106 μm after 3 w of exposure were found as %32 and %35 under RH_{70} and RH_{10}, respectively, while the crystallinities of %37 and %39 were observed for particles with d_p = 400 μm exposed to the UVA radiation for 3 w under similar relative humidity conditions. This finding demonstrates the greater photodegradation of larger particles, as confirmed by the ATR-FTIR results. As shown in Fig. 7, the melting peak temperature for photodegraded MPs was not significantly different from the new samples. This finding indicates that the crystalline phase's structural characteristic and the crystallite's perfection have remained unchanged upon UVA exposure (Dehbi et al., 2010; Miyagawa et al., 2007). In fact, it is anticipated that crystalline zones remain unchanged as degradation mainly occurs in the amorphous areas (Roy et al., 2007). On the other hand, the broader and more intense peaks exhibited by the photodegraded samples indicate the increased crystallinity due to the UVA exposure. Increasing the crystallinity percentage can be described by a phenomenon called secondary crystallization. In essence, polymer backbone cleavage happens over Norrish Type I and II reactions of chromophores is dominant in the amorphous region. The scission route produces low molecular weight segments with two sides available to reorganize or act as nucleating agents leading to an increase in crystallinity. Thus, the secondary crystallization of the small amorphous chain sectors originating from chain scission reactions results in increasing the melting point and crystallinity (Babaghayou et al., 2016; Singh and Sharma, 2008; Sebaa et al., 1993). The chain scission can be recognized by the growth of vinyl groups followed by a reduction in average molecular weight (Babaghayou et al., 2016; Hamid and Amin, 1995). The MPs photodegraded under elevated relative humidity (RH_{70}) demonstrated a lower percentage of increased crystallinity compared to those photodegraded under lower relative humidity (RH_{10}) (Table SI-2). This can be ascribed to a more significant substitution of >C—H bonds with >C═O groups in the samples photodegraded at RH_{10} condition. Several studies reported that increasing the carbonyl group formation is in correlation with an increase in crystallinity, which agrees with our finding presented in the ATR-FTIR Spectroscopy section (Dilara and Briassoulis, 2000; Sebaa et al., 1993; Roy et al., 2007; Briassoulis et al., 2018).

3.4. Light-matter interaction

The increasing duration of UVA exposure from 3 w to 5 w for LDPE MPs (d_p = 400 μm) resulted in an increased average number of chain scission from 5.4 to 7.4 under lower relative humidity (RH_{10}) conditions. On the other hand, it decreased the average number of chain scission from 13 to 5.5 under elevated relative humidity (RH_{70}) conditions (Table 2). Nevertheless, the 3 w UVA exposed MPs under elevated relative humidity exhibited a greater level of chain scission compared to MPs photodegraded under the lower relative humidity condition. The enhancement of hydroxyl radicals formation under elevated relative humidity is responsible for the polymer degradation and is supported by the reported literature (Copinet et al.,

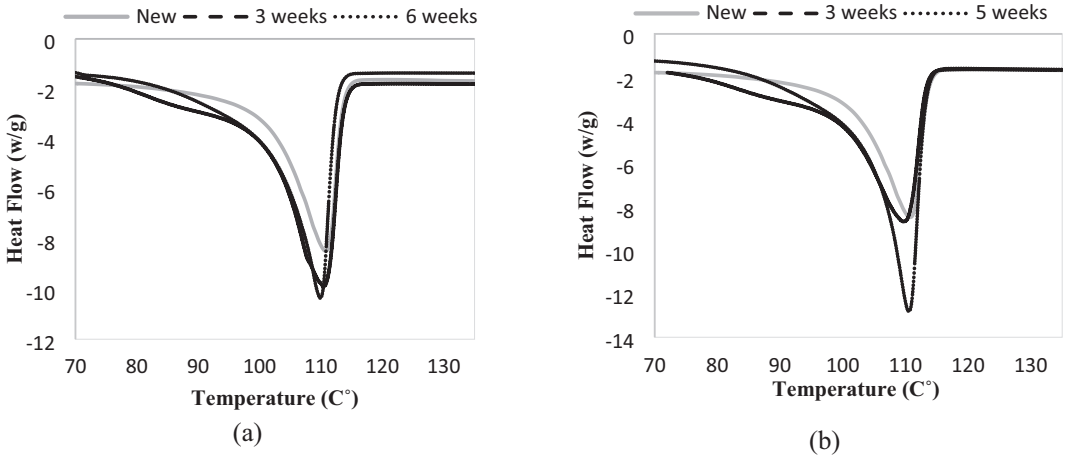

Fig. 7. Endotherm graphs for new and UVA exposed LDPE MPs (400 μm) under (a) RH_{70} and (b) RH_{10}.

Table 2
Chain scission parameters for LDPE MPs.

LDPE MPs	Condition	UVA exposure duration (w)	Average number of chain scission (N)	Intrinsic viscosity (η_{lt})	Quantum yield of chain scission (ϕ_{CS}) × 10^{-2}
d_p = 400 μm	New	0	–	0.7357	–
	RH_{10}	3	5.40	0.2567	3.75
		5	7.43	0.1258	4.79
	RH_{70}	3	13.13	0.2619	5.81
		5	5.47	0.2835	3.50
d_p = 106 μm	New	0	–	0.9582	–
	RH_{10}	5	59.63	0.2970	9.22

2004; James et al., 2013). Besides that, the reduction of chain scissions due to the longer UVA exposure durations could reverse the process as the excited state species abstract protons from water molecules, thus reducing the free radical propagation within the polymer structure (Tjandraatmadja et al., 2002; Laboratories and Hill, 1985). This resulted in an increasing the quantum yield of the chain scission for the LDPE MPs photodegraded under lower relative humidity conditions. As LDPE molecular weight reduces due to chain scission, a rapid decrease in intrinsic viscosity was also found for LDPE MPs photodegraded for shorter UV exposure duration (3 w) from 0.7357 to 0.2567 and 0.2619 dL/g under RH_{10} and RH_{70} conditions, respectively. It is attributed to the weak bond scission caused by reactive oxygen species formed in the presence of oxygen. The LDPE MPs' intrinsic viscosity was further reduced by increasing the UVA exposure duration to 5 w under RH_{10}; however, it slightly increased for LDPE MPs photodegraded under RH_{70}. These findings confirm that the polymer branching and crosslinking predominates over chain scission at longer UVA exposure durations under elevated relative humidity conditions. The MPs (d_p = 106 μm) that were UVA exposed for 3 w at RH_{10} demonstrated the greatest number of polymeric chain sessions (n = 60). However, the obtained result is inconsistent with the result from ATR-FTIR spectrum, as the greatest CI value was found for MPs of d_p = 400 μm. This discrepancy can be explained by the fact that chain scission can occur without the creation of carbonyl groups. Indeed, the polymer breakdown process which occurs due to polymeric chain scissions with a slight increase in CI, indicates that the reactions that lead to carbonyl production are hindered or blocked. On the other hand, the remarkable formation of carbonyl groups with a low number of chain scissions suggests that the polymer degradation is controlled by the oxidation process (Berlanga-Duarte et al., 1996).

4. Conclusion

This study evaluated the sustainability of agricultural plastic products by investigating the combined influence of polymer characteristics and environmental conditions on microplastic aging through accelerated UVA experiments. The results demonstrated that both environmental conditions and polymer intrinsic features influence MPs photodegradation within the environment. The greater relative humidity and deposition of MPs under the soil particles reduced the extent of photodegradation by lowering the available oxygen and inhibiting UVA exposure. However, the photodegradation behavior of MPs that existed within the uniform mixture of the MPs/soil was not different from those irradiated in the absence of soil particles. The MPs with a lower molecular weight were less photostable than those with high molecular weight. The MPs' crystallinity was increased; however, their molecular weights were reduced as a function of UVA exposure duration. This applied research study informs the public, farmers, industry stakeholders, and policymakers regarding the sustainability and eventual fate of agricultural plastic products within the farmland. In addition, the results are illuminating for the plastic industries, wastewater treatment plants, and biosolid distributors regarding the possible long-term soil health impacts associated with the implementation of their product. Food production sustainability and soil functionality are critical objectives for policymakers. Thus, the policymakers may utilize this information to modify and shape regulations and monitoring practices to sustain and improve a healthy and productive farm soil ecosystem.

CRediT authorship contribution statement

Reza Bonyadinejad: Methodology, Investigation, Writing original draft, Visualization.

Maryam Salehi: Conceptualization, Methodology, Resources, Writing, Review and Editing, Supervision.

Amali Herath: Investigation.

Declaration of competing interest

The authors declare that they have no known competing financial interests or personal relationships that could have appeared to influence the work reported in this paper.

Acknowledgment

The authors would like to thank Dr. Farhad Jazaei for his recommendations regarding the methodology, Dr. Felio Perez, and Dr. Omar Skalli for assisting with SEM and XPS analysis. Funding for this work was provided by the United States Department of Agriculture, National Institute of Food and Agriculture (USDA/NIFA) Award number 2020-67019-31166, and National Science Foundation grant CBET-2044836. The authors thank Dr. Tomoko Fujiwara for providing access to the DSC instrument and Dr. Dave DeSimone for assisting with DSC analysis.

Appendix A. Supplementary data

Supplementary data to this article can be found online at https://doi.org/10.1016/j.scitotenv.2022.156385.

References

Aghilinasrollahabadi, K., Salehi, M., Fujiwara, T., 2021. Investigate the influence of microplastics weathering on their heavy metals uptake in stormwater. J. Hazard. Mater. 408, 124439. https://doi.org/10.1016/j.jhazmat.2020.124439.

Ali, S.S., Qazi, I.A., Arshad, M., Khan, Z., Voice, T.C., Mehmood, C.T., 2016. Photocatalytic degradation of low density polyethylene (LDPE) films using titania nanotubes. Environ. Nanotechnology, Monit. Manag. 5, 44–53. https://doi.org/10.1016/j.enmm.2016.01.001.

Angulo-Sanchez, J.L., Ortega-Ortiz, H., Sanchez-Valdes, S., 1994. Photodegradation of polyethylene films formulated with a titanium-based photosensitizer and titanium dioxide pigment. J. Appl. Polym. Sci. 53 (7), 847–856. https://doi.org/10.1002/app.1994.070530702.

Colin, X., Verdu, J., 2012. Aging of organic matrix composite materials. Arts Science Arts & Métiers.

Babaghayou, M.I., Mourad, A.H.I., Lorenzo, V., de la Orden, M.U., Urreaga, J.M., Chabira, S.F., Sebaa, M., 2016. Photodegradation characterization and heterogeneity evaluation of the exposed and unexposed faces of stabilized and unstabilized LDPE films. Mater. Des. 111, 279–290.

Barnes, P.W., Throop, H.L., Hewins, D.B., Abbene, M.L., Archer, S.R., 2012. Soil coverage reduces photodegradation and promotes the development of soil-microbial films on dryland leaf litter. Ecosystems 15 (2), 311–321. https://doi.org/10.1007/s10021-011-9511-1.

Berlanga-Duarte, M.L., Angulo-Sánchez, J.L., González-Cantú, M.C., 1996. Study of polyethylene photodegradation in formulations with a system of interacting photostabilizers and antioxidants. J. Appl. Polym. Sci. 60 (3), 413–424. https://doi.org/10.1002/(sici)1097-4628(19960418)60:3<413::aid-app15>3.3.co;2-7.

Briassoulis, D., Hiskakis, M., Tserotas, P., 2018. Combined effect of UVA radiation and agrochemicals on the durability of agricultural multilayer films. Polym. Degrad. Stab. 154, 261–275. https://doi.org/10.1016/j.polymdegradstab.2018.06.012.

Canopoli, L., Coulon, F., Wagland, S.T., 2020. Degradation of excavated polyethylene and polypropylene waste from landfill. Sci. Total Environ. 698. https://doi.org/10.1016/j.scitotenv.2019.134125.

Copinet, A., Bertrand, C., Govindin, S., Coma, V., Couturier, Y., 2004. Effects of ultraviolet light (315 nm), temperature and relative humidity on the degradation of polylactic acid plastic films. Chemosphere 55 (5), 763–773. https://doi.org/10.1016/j.chemosphere.2003.11.038.

Corradini, F., Meza, P., Eguiluz, R., Casado, F., Huerta-Lwanga, E., Geissen, V., 2019. Evidence of microplastic accumulation in agricultural soils from sewage sludge disposal. Sci. Total Environ. 671, 411–420. https://doi.org/10.1016/j.scitotenv.2019.03.368.

David, C., Trojan, M., Daro, A., Demarteau, W., 1992. Photodegradation of polyethylene: comparison of various photoinitiators in natural weathering conditions. Polym. Degrad. Stab. 37 (3), 233–245. https://doi.org/10.1016/0141-3910(92)90165-2.

de Souza Machado, A.A., Kloas, W., Zarfl, C., Hempel, S., Rillig, M.C., 2018. Microplastics as an emerging threat to terrestrial ecosystems. Glob. Chang. Biol. 24 (4), 1405–1416. https://doi.org/10.1111/gcb.14020.

Dehbi, A., Bouaza, A., Hamou, A., Youssef, B., Saiter, J.M., 2010. Artificial ageing of tri-layer polyethylene film used as greenhouse cover under the effect of the temperature and the UV-A simultaneously. Mater. Des. 31 (2), 864–869. https://doi.org/10.1016/j.matdes.2009.07.047.

Dilara, P.A., Briassoulis, D., 2000. Degradation and stabilization of low-density polyethylene films used as greenhouse covering materials. J. Agric. Eng. Res. 76 (4), 309–321. https://doi.org/10.1006/jaer.1999.0513.

Egerton, T.A., 2014. Uv-absorption-the primary process in photocatalysis and some practical consequences. Molecules 19 (11), 18192–18214. https://doi.org/10.3390/molecules191118192.

FAO, 2021. Assessment of agricultural plastics and their sustainability: A call for action. https://doi.org/10.4060/cb7856en Rome.

Gallo, F., et al., 2018. Marine litter plastics and microplastics and their toxic chemicals components : the need for urgent preventive measures. Environ. Sci. Eur. 30 (13), 1–14. https://doi.org/10.1186/s12302-018-0139-z.

Gewert, B., Plassmann, M.M., Macleod, M., 2015. Pathways for degradation of plastic polymers floating in the marine environment. Environ Sci Process Impacts 17 (9), 1513–1521. https://doi.org/10.1039/c5em00207a.

Goh, E.G., Xu, X., McCormick, P.G., 2014. Effect of particle size on the UV absorbance of zinc oxide nanoparticles. Scr. Mater. 78–79, 49–52. https://doi.org/10.1016/j.scriptamat.2014.01.033.

Guillet, J.E., 1973. The role of energy transfer in the stabilization of polymers. Pure Appl. Chem. 36 (1–2), 127–140. https://doi.org/10.1351/pac197336010127.

Guillet, J.E., Dan, E., 1973. Photochemistry of ketone polymers. X. Chain scission reactions in the solid state. Macromolecules 6 (2), 230–235. https://doi.org/10.1021/ma60032a016.

Hadiuzzaman, M., Salehi, M., Fujiwara, T., 2022. Plastic litter fate and contaminant transport within the urban environment, photodegradation, fragmentation, and heavy metal uptake from storm runoff. Environ. Res. 212 (PA), 113183. https://doi.org/10.1016/j.envres.2022.113183.

Hamid, S.H., Amin, M.B., 1995. Lifetime prediction of polymers. J. Appl. Polym. Sci. 55 (10), 1385–1394. https://doi.org/10.1002/app.1995.070551003.

Horton, A.A., Walton, A., Spurgeon, D.J., Lahive, E., Svendsen, C., 2017. Microplastics in freshwater and terrestrial environments: evaluating the current understanding to identify the knowledge gaps and future research priorities. Sci. Total Environ. 586, 127–141. https://doi.org/10.1016/j.scitotenv.2017.01.190.

Huang, J., Hartemink, A.E., 2020. Soil and environmental issues in sandy soils. Earth-Sci. Rev. 208 (July), 103295. https://doi.org/10.1016/j.earscirev.2020.103295.

Huang, A.J.W.Xiangning, Zemlyanov, Dmitry Y., Diaz-Amaya, Susana, Salehi, Maryam, Stanciu, Lia, 2019. Competitive heavy metal adsorption onto new and aged polyethylene under various drinking water conditions. J. Hazard. Mater. 385, 12158.

Hüffer, T., Metzelder, F., Sigmund, G., Slawek, S., Schmidt, T.C., Hofmann, T., 2019. Polyethylene microplastics influence the transport of organic contaminants in soil. Sci. Total Environ. 657, 242–247. https://doi.org/10.1016/j.scitotenv.2018.12.047.

Isari, E.A., Papaioannou, D., Kalavrouziotis, I.K., Karapanagioti, H.K., 2021. Microplastics in agricultural soils: a case study in cultivation of watermelons and canning tomatoes. Water (Switzerland) 13 (16). https://doi.org/10.3390/w13162168.

James, S.L., Robinson, A.J., Arnold, J.C., Worsley, D.A., 2013. The effects of humidity on photodegradation of poly(vinyl chloride) and polyethylene as measured by the CO2 evolution rate. Polym. Degrad. Stab. 98 (2), 508–513. https://doi.org/10.1016/j.polymdegradstab.2012.12.007.

Jiang, X.J., Liu, W., Wang, E., Zhou, T., Xin, P., 2017. Residual plastic mulch fragments effects on soil physical properties and water flow behavior in the Minqin Oasis, northwestern China. Soil Tillage Res. 166, 100–107. https://doi.org/10.1016/j.still.2016.10.011.

Jung, M.R., et al., 2018. Validation of ATR FT-IR to identify polymers of plastic marine debris, including those ingested by marine organisms. Mar. Pollut. Bull. 127 (December), 704–716. https://doi.org/10.1016/j.marpolbul.2017.12.061 2017.

Kapanen, A., Schettini, E., Vox, G., Itävaara, M., 2008. Performance and environmental impact of biodegradable films in agriculture: a field study on protected cultivation. J. Polym. Environ. 16 (2), 109–122. https://doi.org/10.1007/s10924-008-0091-x.

Kim, S.W., An, Y.J., 2019. Soil microplastics inhibit the movement of springtail species. Environ. Int. 126 (March), 699–706. https://doi.org/10.1016/j.envint.2019.02.067.

Kockler, J., Oelgemöller, M., Robertson, S., Glass, B.D., 2014. Influence of titanium dioxide particle size on the photostability of the chemical UV-filters butyl methoxy dibenzoylmethane and octocrylene in a microemulsion. Cosmetics 1 (2), 128–139. https://doi.org/10.3390/cosmetics1020128.

Laboratories, T.B., Hill, M., 1985. Variables on Degradation Pathways.

Liu, H., et al., 2017. Response of soil dissolved organic matter to microplastic addition in chinese loess soil. Chemosphere 185, 907–917. https://doi.org/10.1016/j.chemosphere.2017.07.064.

Liu, M., et al., 2018. Microplastic and mesoplastic pollution in farmland soils in suburbs of Shanghai, China. Environ. Pollut. 242, 855–862. https://doi.org/10.1016/j.envpol.2018.07.051.

Manos, G., Garforth, A., Dwyer, J., 2000. Catalytic degradation of high-density polyethylene over different zeolitic structures. Ind. Eng. Chem. Res. 39, 1198–1202. https://doi.org/10.1021/ie990512q.

Mccormick, A.R., Hoellein, T.J., London, M.G., Hittie, J., Scott, J.W., Kelly, J.J., 2016. Microplastic in surface waters of urban rivers : concentration, sources, and associated bacterial assemblages. Ecosphere 7 (11), 1–22.

Miyagawa, E., Tokumitsu, K., Tanaka, A., Nitta, K.Hei, 2007. Mechanical property and molecular weight distribution changes with photo- and chemical-degradation on LDPE films. Polym. Degrad. Stab. 92 (10), 1948–1956. https://doi.org/10.1016/j.polymdegradstab.2007.05.019.

Ng, E.L., et al., 2018. An overview of microplastic and nanoplastic pollution in agroecosystems. Sci. Total Environ. 627, 1377–1388. https://doi.org/10.1016/j.scitotenv.2018.01.341.

Petersen, C.T., Hansen, E., Larsen, H.H., Hansen, L.V., Ahrenfeldt, J., Hauggaard-Nielsen, H., 2016. Pore-size distribution and compressibility of coarse sandy subsoil with added biochar. Eur. J. Soil Sci. 67 (6), 726–736. https://doi.org/10.1111/ejss.12383.

Picuno, P., Mugnozza, G.S., 1994. The management of agricultural plastic film wastes in Italy. Proceedings of the Interanational Agricultural Engineering Conference, pp. 797–808.

Ranjan, V.P., Goel, S., 2019. Degradation of low-density polyethylene film exposed to UV radiation in four environments. J. Hazard. Toxic Radioact. Waste 23 (4), 04019015. https://doi.org/10.1061/(asce)hz.2153-5515.0000453.

Richard, H., Carpenter, E.J., Komada, T., Palmer, P.T., Rochman, C.M., Sep. 2019. Biofilm facilitates metal accumulation onto microplastics in estuarine waters. Sci. Total Environ. 683, 600–608. https://doi.org/10.1016/j.scitotenv.2019.04.331.

Rillig, M.C., 2012. Microplastic in terrestrial ecosystems and the soil? Environ. Sci. Technol. 46 (12), 6453–6454. https://doi.org/10.1021/es302011r.

Rodriguez, A.K., Mansoor, B., Ayoub, G., Colin, X., Benzerga, A.A., 2020. Effect of UV-aging on the mechanical and fracture behavior of low density polyethylene. Polym. Degrad. Stab. 180. https://doi.org/10.1016/j.polymdegradstab.2020.109185.

Roff, W.J., 1956. Fibres, Plastics and Rubbers. Butterworths Scientific Publications, London.

Roy, P.K., Surekha, P., Rajagopal, C., Chatterjee, S.N., Choudhary, V., 2007. Studies on the photo-oxidative degradation of LDPE films in the presence of oxidised polyethylene. Polym. Degrad. Stab. 92 (6), 1151–1160. https://doi.org/10.1016/j.polymdegradstab.2007.01.010.

Salehi, M., Jafvert, C.T., Howarter, J.A., Whelton, A.J., 2018. Investigation of the factors that influence lead accumulation onto polyethylene : implication for potable water plumbing pipes. J. Hazard. Mater. 347, 242–251. https://doi.org/10.1016/j.jhazmat.2017.12.066.

Sebaa, M., Servens, C., Pouyet, J., 1993. Natural and artificial weathering of low-density polyethylene (LDPE): calorimetric analysis. J. Appl. Polym. Sci. 47 (11), 1897–1903. https://doi.org/10.1002/app.1993.070471101.

Shah, A.A., Hasan, F., Hameed, A., Ahmed, S., 2008. Biological degradation of plastics: a comprehensive review. Biotechnol. Adv. 26 (3), 246–265. https://doi.org/10.1016/j.biotechadv.2007.12.005.

Singh, B., Sharma, N., 2008. Mechanistic implications of plastic degradation. Polym. Degrad. Stab. 93 (3), 561–584. https://doi.org/10.1016/j.polymdegradstab.2007.11.008.

Song, Y.K., Hong, S.H., Jang, M., Han, G.M., Jung, S.W., Shim, W.J., 2017. Combined effects of UV exposure duration and mechanical abrasion on microplastic fragmentation by polymer type. Environ. Sci. Technol. 51 (8), 4368–4376. https://doi.org/10.1021/acs.est.6b06155.

Steinmetz, Z., 2016. Plastic mulching in agriculture. Trading short-term agronomic benefits for long-term soil degradation?. Elsevier B.VSci. Total Environ. 550, 690–705. https://doi.org/10.1016/j.scitotenv.2016.01.153 Apr. 15.

Tjandraatmadja, G.F., Burn, L.S., Jollands, M.C., 2002. Evaluation of commercial polycarbonate optical properties after QUV-A radiation - the role of humidity in photodegradation. Polym. Degrad. Stab. 78 (3), 435–448. https://doi.org/10.1016/S0141-3910(02)00179-9.

Wagner, M., Lambert, S., Contaminants, E.E., 2018. Freshwater Microplastics. Springer Nature, Switzerland.

Wan, Y., Wu, C., Xue, Q., Hui, X., 2019. Effects of plastic contamination on water evaporation and desiccation cracking in soil. Sci. Total Environ. 654, 576–582. https://doi.org/10.1016/j.scitotenv.2018.11.123.

Zahra, Y., et al., 2014. Thermo-oxidative aging of epoxy coating systems. Prog. Org. Coat. 77 (2), 380–387.

Zhang, G.S., Zhang, F.X., Li, X.T., 2019. Effects of polyester microfibers on soil physical properties: perception from a field and a pot experiment. Sci. Total Environ. 670, 1–7. https://doi.org/10.1016/j.scitotenv.2019.03.149.